

# ASSESSMENT OF GROUNDWATER POTENTIAL ZONES BY USING GEOSPATIAL TECHNIQUES IN NANDANI RIVER BASIN, WESTERN MAHARASHTRA, INDIA

## Abstract

The present study focused on the groundwater assessment for Nandani watershed using remote sensing and GIS techniques. The Nandani watershed has covered an area of 492 km<sup>2</sup>. For this study, all the satellite data is obtained from Bhuvan website and analyzed in ArcGIS software. The groundwater potential zones have been delineated using remote sensing and GIS techniques. About 48% area comes under high potential zone, 43% area comes under moderate potential zone and 9% area comes under poor and very poor potential zone. The preparation of different thematic layers such as lithology, slope, land-use, lineament, drainage, soil, and rainfall is facilitated by employing Survey of India toposheets and LISS III satellite images. These diverse factors are converted into raster data through the utilization of the feature to raster converter tool within the ArcGIS software. To assign significance, raster maps representing these factors are given predetermined scores and weights, calculated using the multi influencing factor (MIF) technique. The resulting output holds significant utility in promoting effective watershed development and water resource planning.

**Keywords:** Watershed, Arcgis, Groundwater Assessment.

## Authors

### **Pavan Lokare**

Assistant Professor  
Department of Civil Engineering  
Dr. Daulatrao Aher College of  
Engineering, Karad, India.  
pavanlokare78@gmail.com

### **Abhijit Zende**

Head of Department and Professor  
Department of Civil Engineering  
Dr. Daulatrao Aher College of  
Engineering, Karad, India.

## I. INTRODUCTION

Groundwater stands as a crucial natural asset, ensuring secure and economically accessible drinking water in both urban and rural settings. Its significance extends to the well-being of human populations, as well as certain aquatic and terrestrial ecosystems. Currently, groundwater accounts for approximately 34% of the total annual water supply, serving as a vital freshwater resource. Therefore, evaluating this resource holds immense importance in maintaining sustainable groundwater systems. Leveraging GIS and remote sensing tools has become a prevalent method for managing various natural resources, as noted by Magesh et al. (2011). Utilizing remote sensing and GIS to delineate potential groundwater zones proves to be an effective approach. In recent times, the combination of satellite data, traditional maps, and verified ground information has simplified the establishment of foundational data for groundwater potential zones (Tiwari and Rai, 1996; Thomas et al., 1999; Chowdhury et al., 2010). Notably, remote sensing not only offers comprehensive spatiotemporal observations but also yields time and cost savings (Tweed et al., 2007). It is also widely employed for characterizing surface features like lineaments, drainage patterns, lithology, and assessing groundwater recharge areas (Sener et al., 2005).

Researchers worldwide engage in utilizing remote sensing and GIS to explore groundwater potential zones, revealing variations in determining factors and consequently, diverse outcomes. Teeuw (1995) focused solely on lineaments for groundwater assessment, while others amalgamated factors such as drainage density, geomorphology, geology, slope, land-use, rainfall intensity, and soil texture. The outcomes derived from these efforts, validated through field surveys, exhibit regional variability due to distinct geo-environmental conditions.

Groundwater development in the studied area involves the establishment of dug wells, dug-cum-bore wells, and bore wells. However, the replenishment of these groundwater sources faces challenges posed by recurring dry periods and monsoon failures. Over recent decades, the exploitation of groundwater resources has surged, leading to excessive consumption and resulting ecological issues like declining groundwater levels, resource depletion, water contamination, and compromised water quality.

Integrating remote sensing and GIS to formulate diverse thematic layers, encompassing factors like lithology, drainage density, lineament density, rainfall, slope, soil, and land-use, with assigned spatial weights, aids in identifying potential groundwater zones. Thus, this study concentrates on pinpointing groundwater potential zones within Tamil Nadu's Theni district, employing advanced techniques such as remote sensing, MIF, and GIS. The objective is to facilitate the planning, utilization, administration, and management of groundwater resources in a comprehensive manner.

## II. STUDY AREA

The Nandani River serves as a prominent tributary of the Yerala River, originating in the elevated terrain of Aundh, Maharashtra, India. Its course traverses the rain shadow zone of Satara and Sangli districts, ultimately meeting the Yerala River at the convergence point near Kadepur village, Sangli. The study area's geographical coordinates range from 16° 55' to 17° 28' N in latitude and 74° 20' to 74° 40' E in longitude. Encompassing an overall expanse

of 492 km<sup>2</sup> (depicted in Figure 1), this watershed exhibits a tropical monsoon climate characterized by consistent temperature, humidity, and evaporation patterns throughout the year. Rainfall primarily occurs during the South-West monsoon period from June to September, although its distribution isn't uniform across the entire region. Notably, July and August witness heightened rainfall leading to substantial runoff. Rainfall stations situated in Karad, Kadegaon, Vita, Palus, and Vaduj contribute data. It's worth noting that around 20% of the total annual rainfall is received post-monsoon, predominantly through thunder showers in May. Temperatures can surge to 44°C in summer and plummet to 20°C during winter. The regional climate falls within the subtropical category, characterized by hot and arid conditions during the summer months.

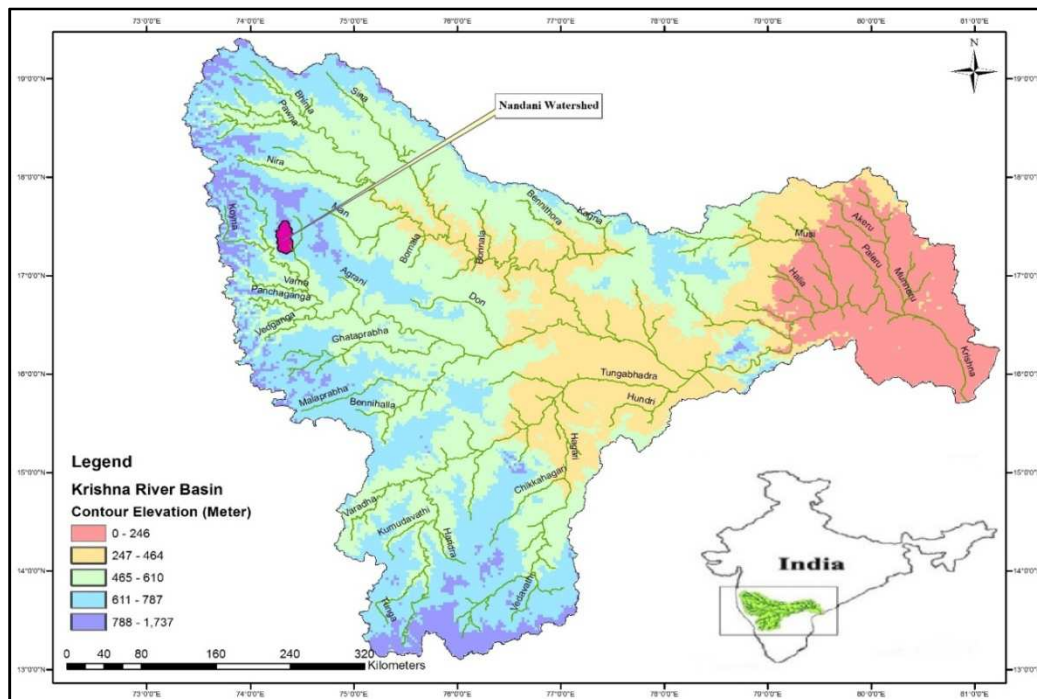


**Figure 1:** Location Map of Nandani Watershed

### III.METHODOLOGY

**1. Generation of Spatial Database:** The initial and fundamental stage of GIS analysis involves inputting spatial data generated from diverse sources. Within this present analysis, a range of maps including drainage network, drainage density, flow direction, flow accumulation, contour map, slope, Land Use/Land Cover, soil, geomorphology, and watershed boundaries were crafted using Survey of India toposheets at a scale of 1:50,000. Satellite data was utilized to update the drainage network map and surface water bodies. The satellite-based drainage network map, depicted in Figure 10, was formulated according to the methodology outlined by Pandey et al. (2008), revealing a dendritic drainage pattern indicative of lithological homogeneity. The application of Strahler's stream ordering (1964) was performed, an essential parameter for soil conservation planning.

A Digital Elevation Model (DEM) boasting a spatial resolution of 200 x 200 meters was derived from digitized contour lines and spot height information across the entire watershed. Subsequently, a slope map was generated from this DEM. Utilizing both the DEM and drainage network, the study area was divided into seven sub-watersheds. The soil map was sourced from Bhuvan.in, digitized using ARC-GIS, and depicted in Figure 7.

In this particular study, the Land Use/Land Cover map was crafted using data from the LISS-III satellite through ERDAS IMAGINE-10.0 digital image processing software. Geo-referencing was initially undertaken by aligning identifiable features like road intersections, railways, canals, and bridges between Survey of India topographical maps and the satellite data. A supervised classification approach within ERDAS IMAGINE 10.0 was employed to create the Land Use/Cover map, after conducting numerous ground truth verifications. These various maps were encoded as GIS layers and standardized to facilitate integrated analysis within the GIS environment. This spatial organization ensured that all encoded digital data shared the same resolution and coordinate system.

The IRS-1C LISS-III satellite image was subjected to supervised classification within the ERDAS IMAGINE software, implementing the maximum likelihood classification algorithm and verifying results against ground truth data. The primary land use classes within the study area include upland crops, forests, and wasteland/fallow land, as depicted in Figure 7. The generation of the land use/cover map involved a supervised classification process based on False Colour composites (FCC).

- 2. Groundwater Potential Zone:** In the realm of groundwater resource mapping and planning, the integration of remote sensing and geographic information systems (GIS) emerges as a promising framework for the comprehensive analysis of diverse datasets. By amalgamating insights obtained from the analysis of multi-source remote sensing data within a GIS framework, the objective is to formulate and implement integrated methodologies that enhance our comprehension of groundwater resources. The spectrum of satellite data products is notably diverse, contingent upon the spectral bands considered. The interpretation of high-resolution satellite imagery, whether through visual or digital means, aids in the identification of potential groundwater zones. These zones are demarcated based on factors such as hydrogeomorphic units, land use, land cover, lineaments, rock types, and geological structures, each contributing to the creation of thematic layers.

Central to the methodology is the delineation of hydrogeomorphic units influenced by the local hydrogeological conditions. Elements like lithology, geomorphology, and geological structures, including lineaments, faults, and fractures, exert a significant influence on these hydrogeological conditions. Priority zones garner focused attention through the visual interpretation of satellite data, complemented by limited field verification of identified features.

In this study, the creation of groundwater prospective zone maps in the study area leveraged hydrological and geomorphological insights derived from enhanced satellite products via both visual and digital analyses. The assessment of groundwater potential

zones hinged on the preparation and integration of various thematic layers within GIS. These thematic layers, encompassing attributes such as lithology, geomorphology, drainage density, lineaments, and slope, were generated from satellite imagery as well as Survey of India (SOI) maps. Given that raw satellite images lack inherent coordinate information, georeferencing was conducted using actual ground reference points from GPS instruments or established survey maps.

To establish groundwater potential zones, the spatial analysis tool within ArcGIS 10.0 was employed, employing weighted overlay methods to superimpose all thematic maps. Within this process, each parameter within a thematic map was assigned a ranking and corresponding weights based on its multi influencing factor (MIF) on the study area's hydrogeological environment during weighted overlay analysis, as outlined by Shaban et al. (2006). A potential zone's overall weight is the cumulative sum of individual weights from each contributing factor. Factors assigned higher weight values exert a more substantial impact on groundwater potential zones, while those with lower weight values hold lesser influence. The ArcGIS software's weighted overlay analysis computes the amalgamation of these factors along with their respective weights.

Various influencing factors for groundwater potential zones—namely lineaments, drainage, lithology, slope, land use, and soil—were evaluated and assigned appropriate weights, detailed in Table 1. The comprehensive methodology is illustrated in Figure 2.

**Table 1: Rank and Weightage of Different Parameters for Groundwater Potential Zones**

Sr. No.	Criteria	Classes	Rank	Weightage (%)
1.	Geology	Phyric Basalt	1	10%
		Megacryst Flow	2	
		Highly Porphyritic Basalt	3	
2.	General Soil Group	Gravelly Clay	1	25%
		Gravelly Clay Loam	2	
		Sandy Clay Loam	3	
3.	Land Use	Agricultural land	1	25%
		Fallow Land	2	
		Open Scrub Land	3	
4.	Slope	0° - 15°	1	15%
		15° - 33°	2	
		> 33°	3	
5.	Lineament	Present	1	5%
		Not Present	2	
6.	Drainage	First order – Second order	1	20%
		Second order – Fourth order	2	
		Fourth order – Sixth Order	3	

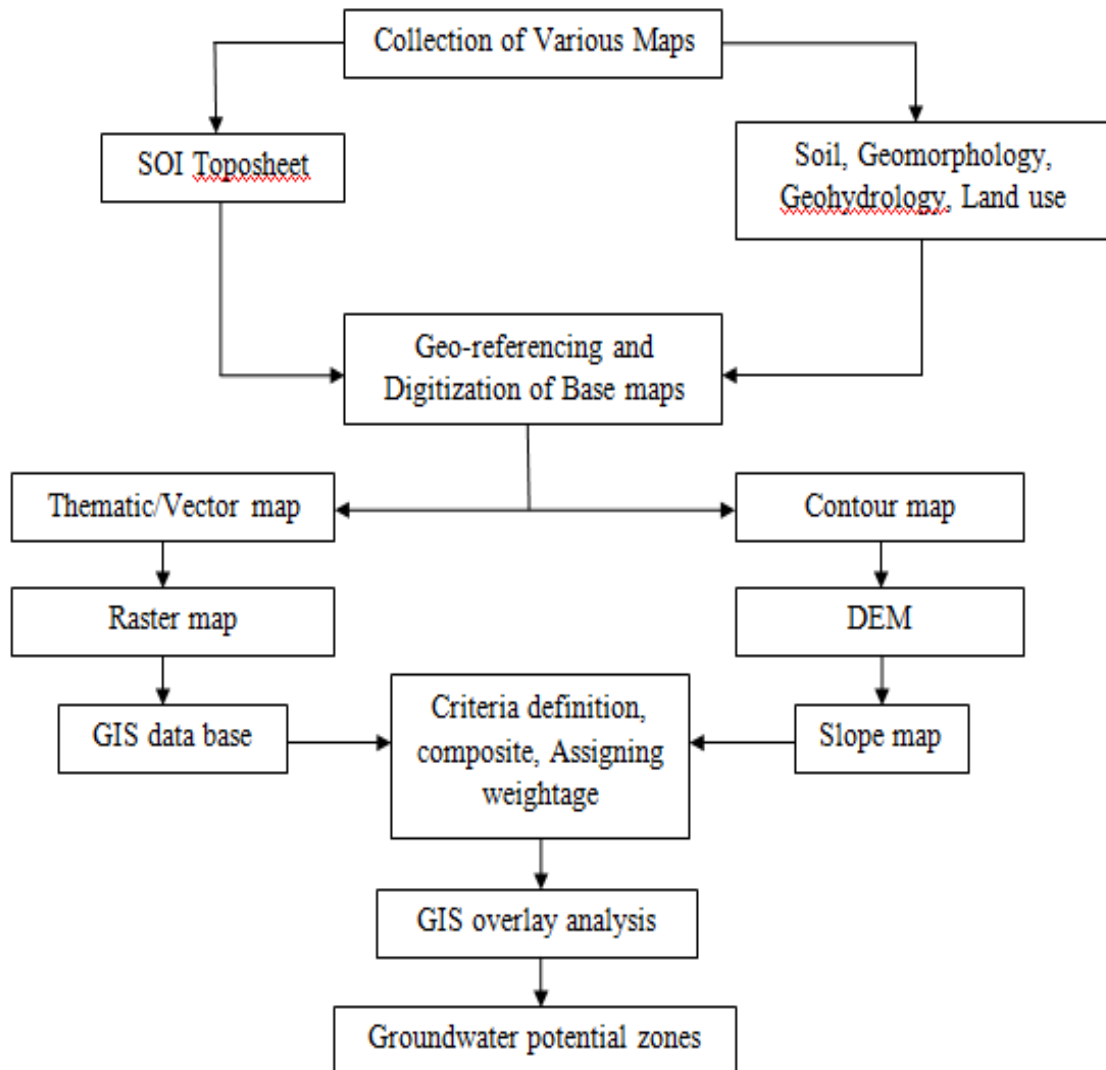


**Figure 2:** Methodology Flowchart

#### IV. RESULTS AND DISCUSSIONS

- 1. Geology:** The geological composition of the area predominantly consists of basaltic rock formations, as demonstrated in Figure 3. Past tectonic movements have left discernible imprints, with various folds, faults, and lineaments associated with the hills situated on the western side of the study area serving as evidence. The region is overlaid by basaltic flows linked to Cretaceous to Eocene Deccan Volcanic activity, earning them the term "Deccan Trap" due to their distinct step-like topography. The thickness of individual flows spans from a few meters to 40 meters, with extensive coverage across the landscape. The mineralogical and chemical composition of the basaltic lava flows remains consistent throughout the study area.

The basaltic flows fall into categories of compact, fine-grained, massive basalt, and vesicular, amygdaloidal basalt. The vesicles in the latter are filled with secondary minerals like quartz, chalcedony, and calcite. The distribution reveals that 81% of the area is covered by phyrlic basalt, 12% by megacryst flow, 7% by highly porphyritic basalt, and less than 1% by basaltic lava, as depicted in Figure 3. Detecting the boundaries of these flows relies on indicators such as the presence of red beds, shifts in jointing and weathering patterns, ropy surfaces, and other distinguishing characteristics. Additionally, the development of level surfaces at varying altitudes serves as an identifier for different basaltic flows, conceptualized as flow tops. Separating these flows are commonly red to brown clayey rock formations known as 'red beds,' varying in thickness from centimeters to over two meters. These formations exhibit a gradient relationship with the upper section of the underlying flow, attaining porosity and permeability through secondary factors such as fracturing and weathering.

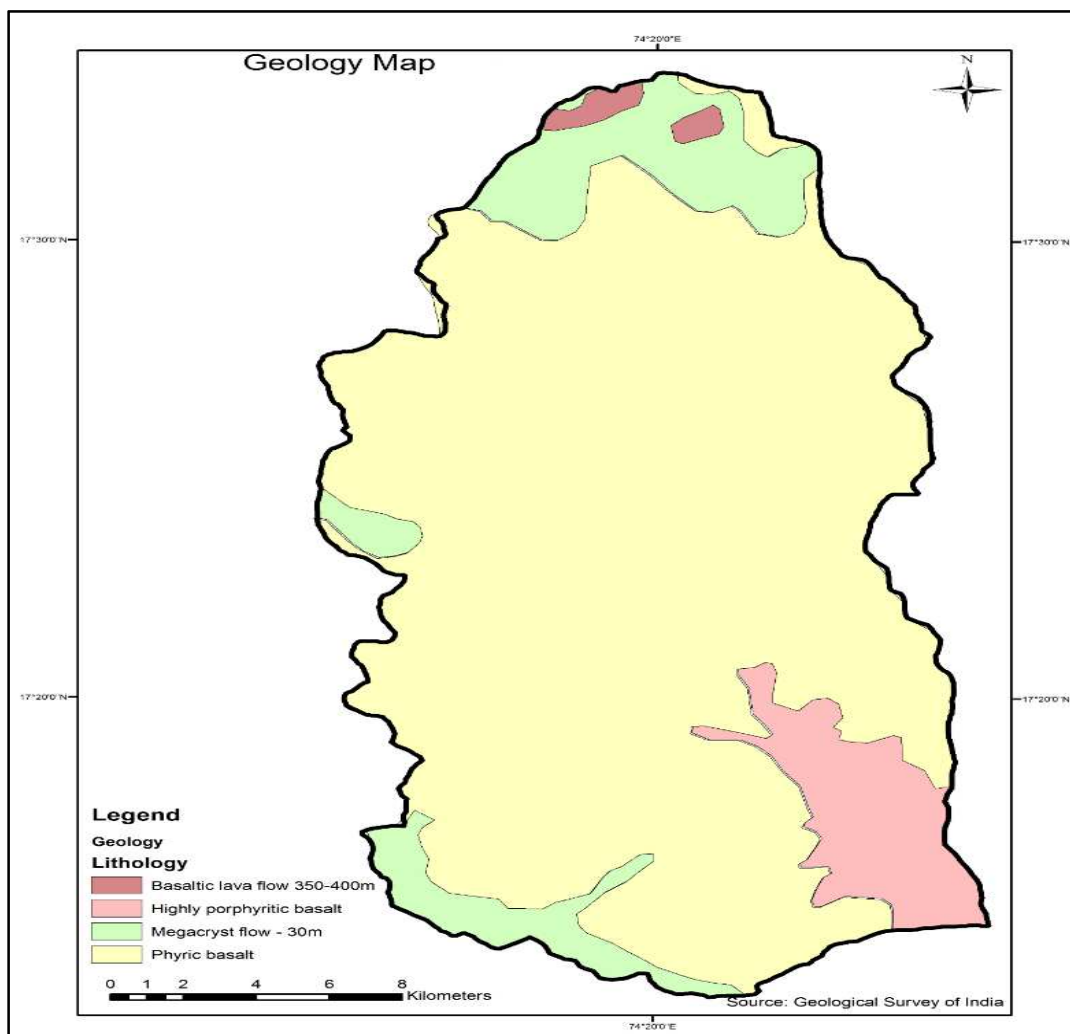


**Figure 3:** Geology Map of Nandani Watershed

In regions characterized by high rainfall and effective drainage, the weathering of basalt leads to the formation of laterite. During this process, elements like silica, alkalis,

and alkaline earths leach away, leaving alumina, iron, manganese, and titanium behind. The structural composition of laterite takes the form of vermiculite or pisolite.

Alluviums present in the area comprise stratified deposits of gravel, sand, silt, and clays that are the result of stream and river deposition. Notably, well-developed alluvial deposits line the banks of major rivers in these districts. These deposits commonly exhibit attributes like graded bedding, current bedding, and cross bedding. At the base of these deposits, finely graded sand and silt coexist with kankar nodules, known locally as Mann.

- 2. Geomorphology:** Geomorphology represents a distinctive terrain configuration that offers valuable insights into the characterization of subsurface groundwater conditions. Within the study area, three distinct geomorphic units have been discerned, visually depicted in Figure 4. The geomorphological landscape of the Nandani Basin is primarily composed of Denudational hills and valleys, Denudational origin areas, and Older Flood Plains. The distribution across the basin is as follows: Denudational hills and valleys cover about 11% (54 km<sup>2</sup>) of the area, Denudational origin encompasses 56% (275.5 km<sup>2</sup>), and Older Flood Plains account for 33% (162.5 km<sup>2</sup>). The Nandani Watershed is further divided into seven designated sub-watersheds.

Geomorphology entails the investigation of landform shapes and the processes that shape them, stemming from an interplay of exogenetic and endogenetic forces. Landforms hold critical significance for tasks such as mapping land resources, conducting watershed studies, evaluating terrain attributes, and classifying soils.

A significant expanse of the basin has evolved on the Deccan Plateau, bounded by the Western and Eastern Ghats, constituting the largest geomorphic sub-unit of the Indian Peninsula. During the late Cretaceous-Eocene period, substantial Deccan volcanic activities transpired across western and central India. These events led to the widespread eruption of basalts, not only submerging the low-relief pre-Trappean landscape but also giving rise to a youthful topography upon which sub-aerial processes took root, leading to the establishment of a novel drainage network. This transformative phase of erosion commenced along the newly formed rifted margin, operating up to the then-existing level of erosion, ultimately shaping the contemporary landforms like the Deccan Plateau and the Western Ghats.

The mountainous regions consist of metamorphosed volcanic rock layers displaying an array of colors such as red, brown, yellow, grey, and white. Within the study area, the western segment is characterized by Denudational hills and valleys, while the middle and eastern sectors are defined by Denudational origin areas and Older Flood Plains. Generally, the terrain gently inclines towards the east, featuring undulating plains. Several parallel ridges comprised of sand, pebbles, and shells rise at relatively elevated altitudes, and the intervening depressions accommodate features like swamps and silts. The distribution and extent of these geomorphic attributes exhibit significant variability based on the underlying geological conditions.

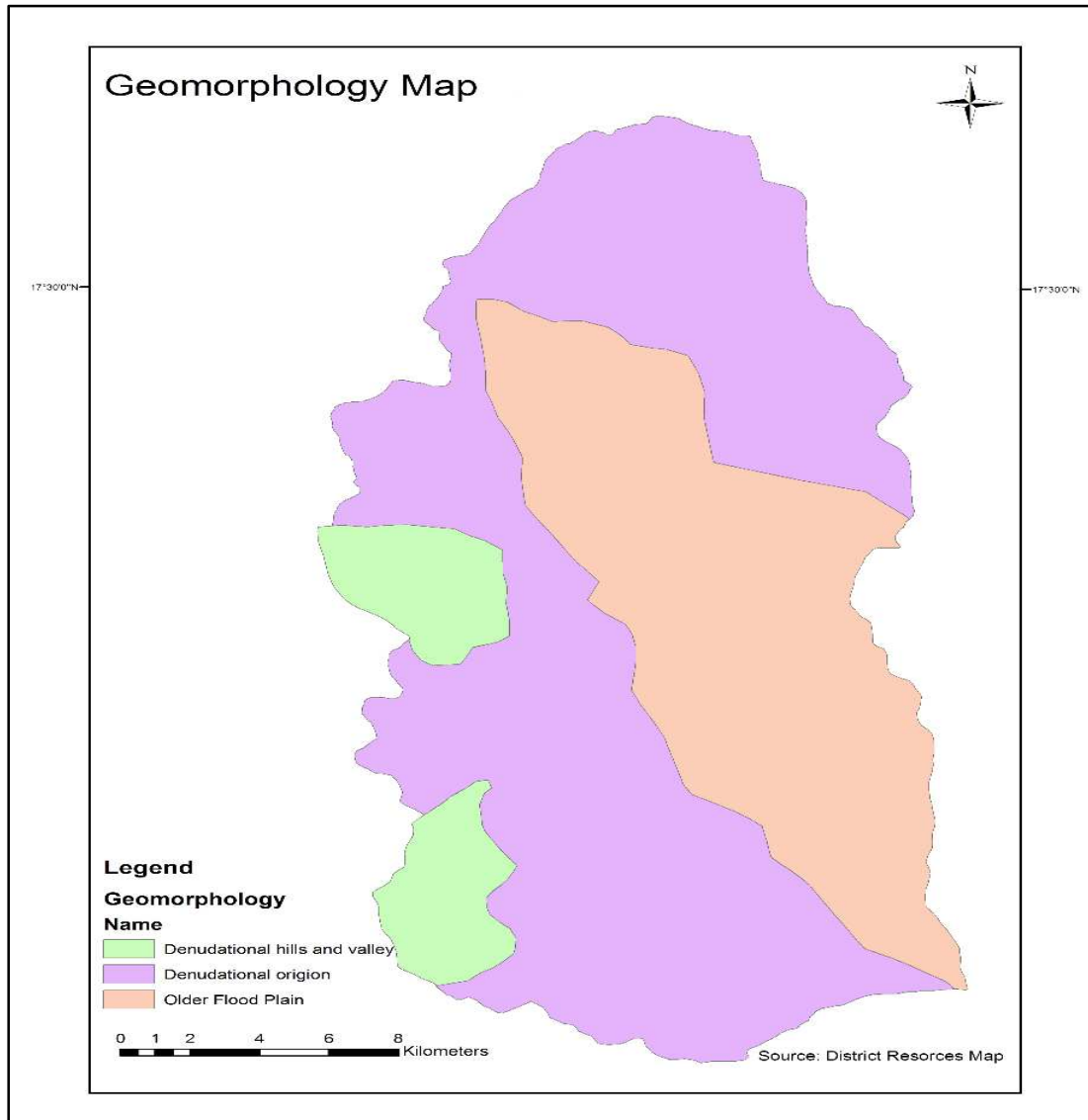


**Figure 4:** Geomorphological Map of Nandani Watershed

- 3. Hydrological Soil Group (HSG):** The soil composition comprises distinct classes, namely gravelly clay soil, gravelly clay loam, sandy clay loam, and gravelly sandy loam. The classification of the hydrologic soil group (HSG) is developed based on the infiltration rate of different soil textures, as derived from the soil map. Correspondingly, the previously mentioned soil classes are categorized into three groups: B, C, and D, as illustrated in Figure 5. The B-type soil extends over 31% of the basin area, the C-type soil encompasses 33% of the basin, and the D-type soil encompasses 36% of the basin. The western segment of the basin area is enveloped by D-type soil, while the northeastern portion is characterized by B-type soil. Out of the total 492 km<sup>2</sup> area, approximately 152.5 km<sup>2</sup> is occupied by B-type soil, 162 km<sup>2</sup> by C-type soil, and 177.5 km<sup>2</sup> by D-type soil.

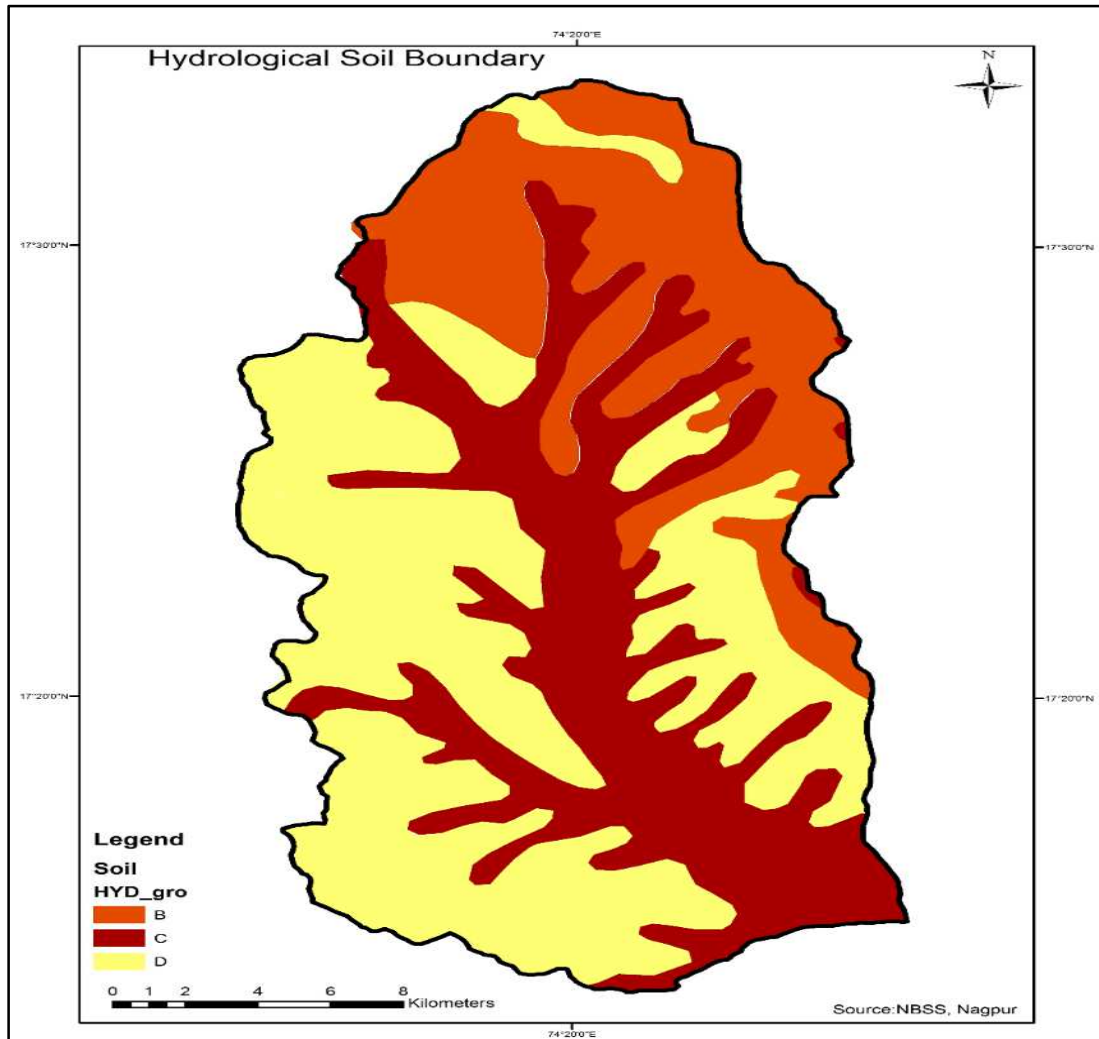


**Figure 5:** Hydrological Soil map of Nandani Watershed

- 4. Land use/ Land Cover:** Multi-date satellite images reveal surface conditions, encompassing aspects like natural vegetation, cultivated regions, water reservoir extent, and various other land cover and land use attributes. Employing the Arc GIS software tool, the area across five distinct categories was determined based on their respective land use and land cover characteristics. The predominant land use types within the study area include agricultural land, open scrub land, fallow land, and water bodies. These categories are demarcated using IRS-P6 LISS-III satellite data, supplemented by rigorous field verification. Five land use/cover classes—namely agricultural land, water bodies, open scrub land, fallow land, and natural vegetation (Figure 7)—were established from four IRS P6 LISS-III satellite images captured in the years 1990, 2015, 2017, and 2018.

Approximately 60.57% of the total area is dedicated to agricultural land, while forest land covers 6.10%, dry land encompasses 18.09%, and the remaining 15.24% is allocated to other uses such as water bodies, hills, settlements, and tanks. To facilitate the interpretation of False Colour Composites and create user-friendly land use/land cover maps, unobstructed FCCs for four different years were acquired from the Bhuvan.Org

website, ensuring cloud-free images. ERDAS IMAGINE 10 software was employed to process satellite images for tasks like visual interpretation, digital image classification, change detection studies, and water assessment analysis. Figure 6 portrays the False Colour Composite of the Nandani watershed captured on 4th January 2018, while Figure 6 presents the Land Use/Land Cover map for the same date.

The entire extent of the Nandani watershed spans 492 km<sup>2</sup>, of which agricultural land occupies approximately 298 km<sup>2</sup>, forest land spans 30 km<sup>2</sup>, dry land covers an area of 89 km<sup>2</sup>, and the remaining 75 km<sup>2</sup> accommodates various other uses such as water bodies, hills, settlements, and tanks.

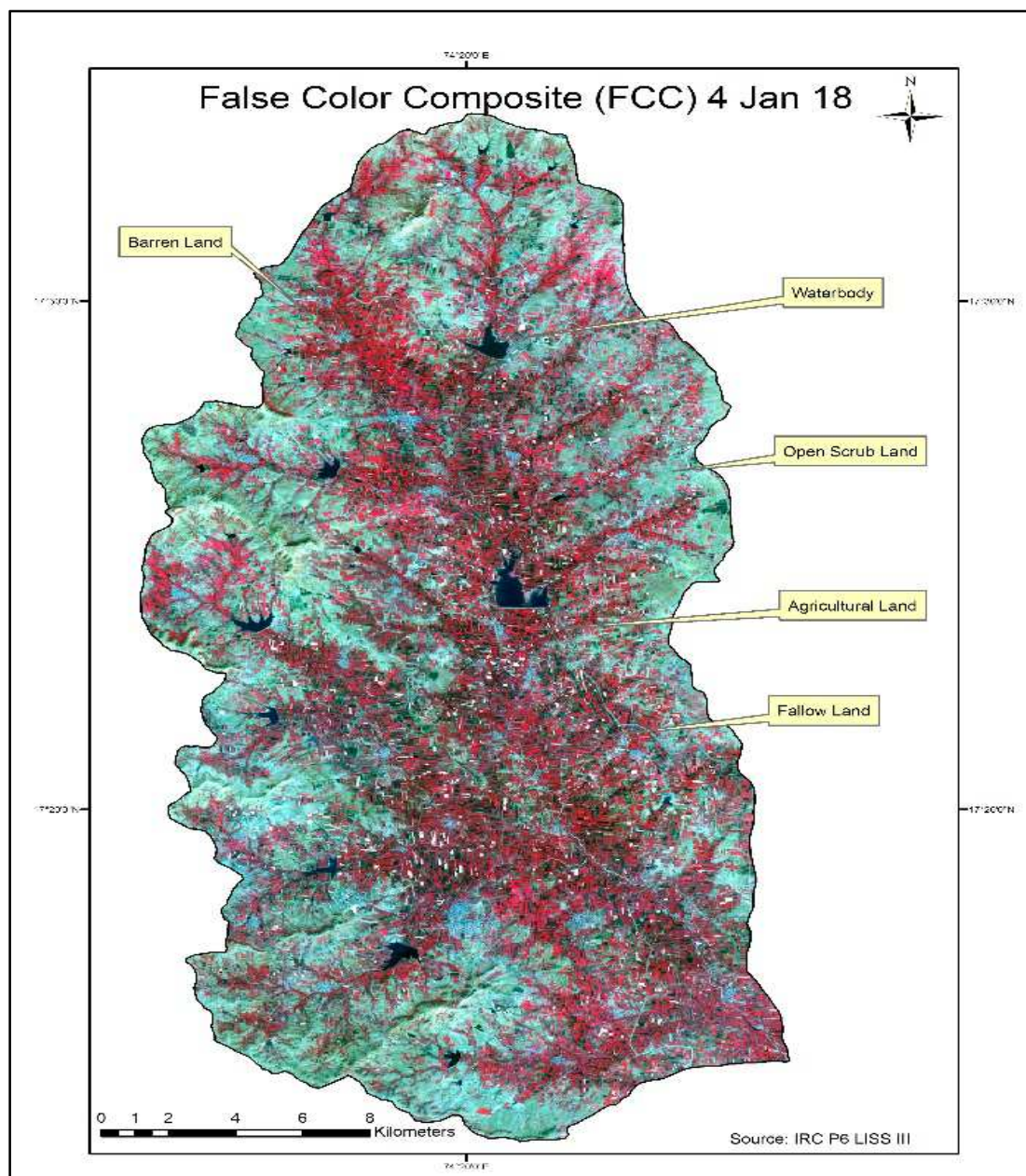


**Figure 6:** False Colour Composite of Nandani Watershed, 4 Jan 2018

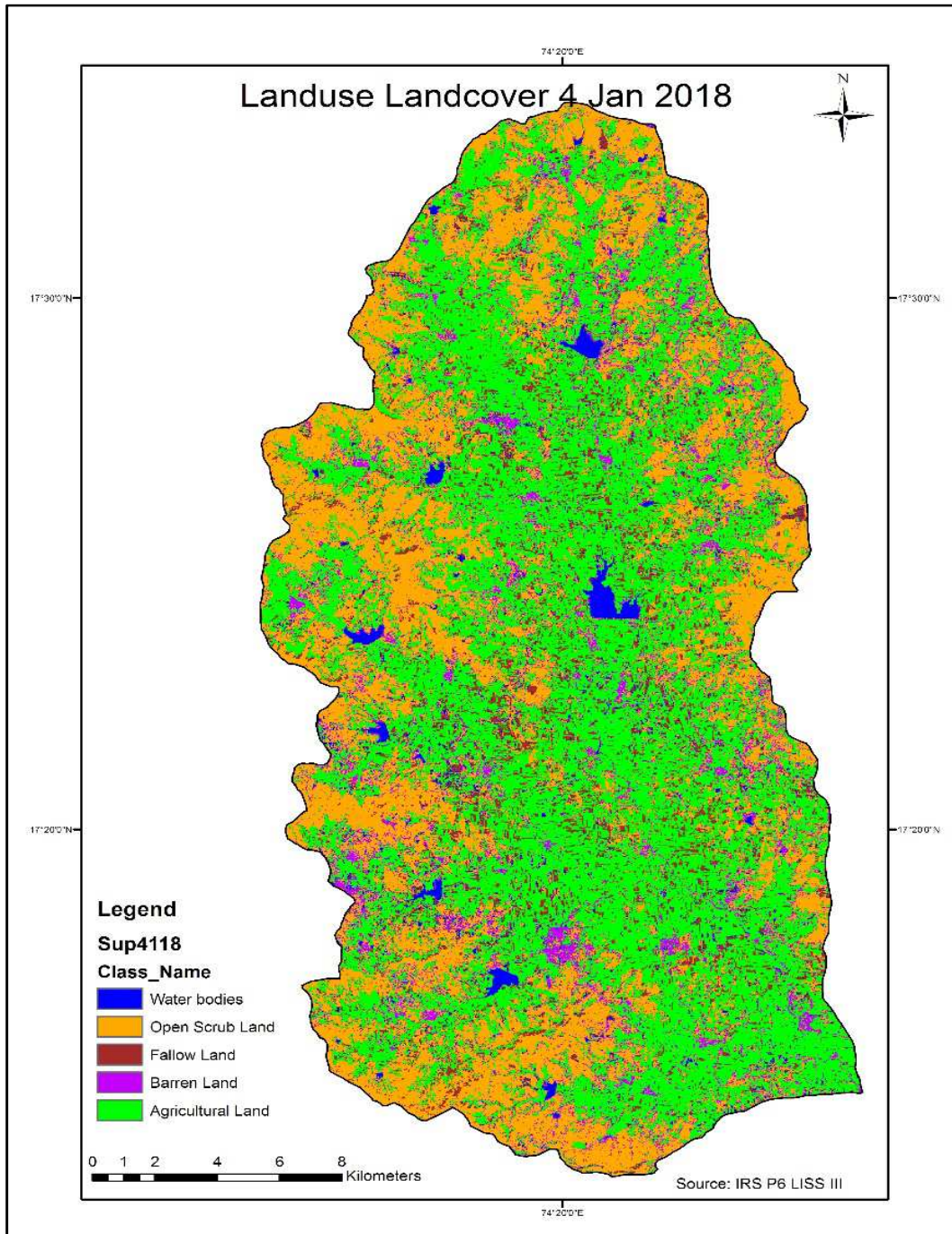


**Figure 7:** Land use Land Cover of Nandani Watershed, 4 Jan 2018

- 5. Slope:** The generation of the slope map is facilitated by utilizing the Digital Elevation Model (DEM). To initiate this process, the contour map is first transformed into the DEM, subsequently leading to the production of the slope map (depicted in Figure 8). This slope map is then subjected to further classification to assess potentially suitable sites for various water harvesting structures. By referring to the slope map, one can examine the appropriateness and positioning of structures in accordance with factors like runoff rate and sedimentation deposition.

The study area is stratified into five distinct slope classes based on the gradient. Locations boasting a slope ranging from 0 to 8 are designated as 'very good,' owing to their nearly flat topography and commendable infiltration rate. Areas with a slightly undulating terrain and notable runoff, encompassing a slope of 9 to 15, are classified as 'good' for groundwater storage. Regions marked by a slope of 16 to 33, exhibiting higher runoff and diminished infiltration, are deemed 'poor.' Finally, those areas showcasing a slope exceeding 33 are categorized as 'very poor,' primarily due to the pronounced incline leading to heightened runoff.

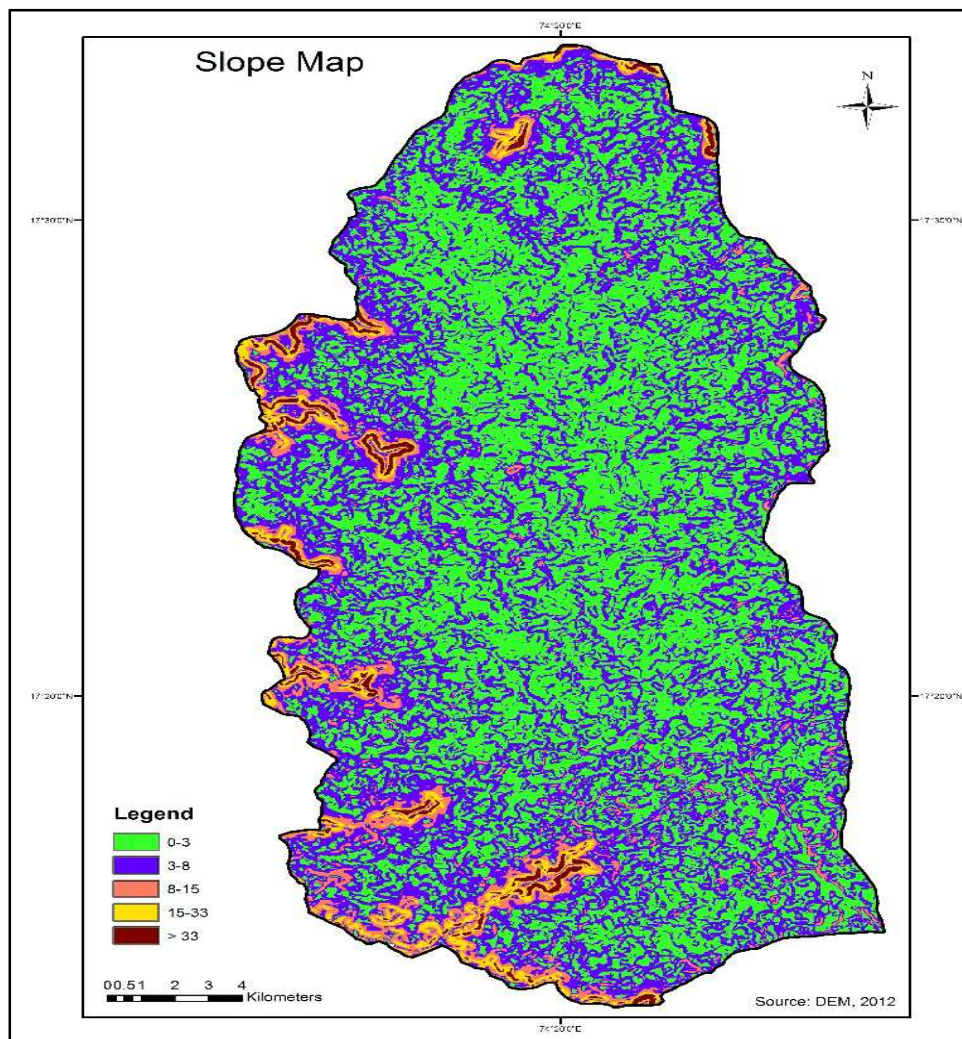


**Figure 8:** Slope Map of Nandani Watershed

- 6. Lineament:** An additional significant aspect to take into account concerning artificial recharge systems is the concept of lineaments. A lineament constitutes a landscape feature that offers insights into an underlying geological structure, encompassing elements like faults, fractures, or joints. Lineaments serve as pivotal elements in the investigation of fractures or structures, utilizing remote sensing techniques. In this study area, the interpretation of lineaments draws from the district resource map and geological

map. The Lineament map of the Nandani Watershed is visually represented in Figure 9. This map reveals a division within the study area, segregating it into two distinct sections: the eastern part and the western part. The presence of lineaments within the study area effectively highlights the course of the main stream, which flows from the northern to the southern direction.

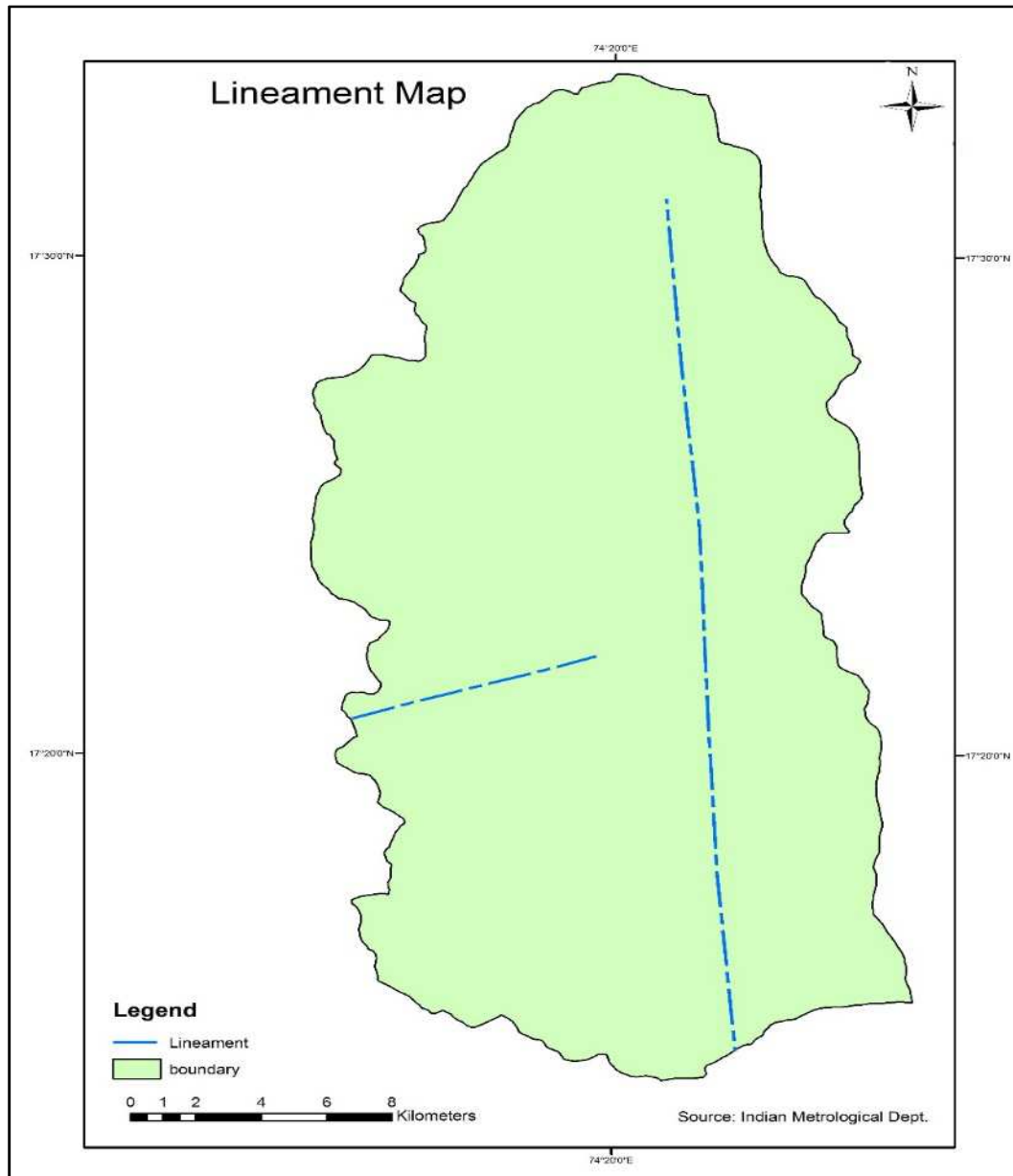


**Figure 9:** Lineament map of Nandani Watershed

- 7. Drainage:** The majority of the Sangli district is drained by the Krishna River and its affluents, including the warna, Morna, Yerala, and Agrani rivers. Parts of Atpadi, Kawthe Mahankal, and Jat taluka are drained by the Man and Bor rivers, which are tributaries of the Bhima river. Except for the Krishna, warna, and Morna rivers, which exhibit perennial flow, all other rivers and streams in the area are seasonal. While the prevailing

drainage pattern is dendritic, localized occurrences of trellis, rectangular, angulate, and subparallel drainage patterns can also be observed.

The total drainage area of the Nandani basin spans 492 km<sup>2</sup>. This drainage pattern adheres to a dendritic arrangement, influenced by the geographical features of the region. Notably, the tributaries of the Nandani river are classified as sixth-order streams. A comprehensive count reveals the presence of 1655 streams, with 1219 categorized as first order, 332 as second order, 77 as third order, 18 as fourth order, 8 as fifth order, and 1 as sixth order. The corresponding drainage map is depicted in Figure 10.

The preparation of the drainage map involves digitizing individual streams from the Survey of India topographic sheets at a scale of 1:50000. These streams are then assigned stream orders in accordance with Strahler's law of stream order (1964). Following this principle, the merging of two first-order streams results in a second-order stream, while two second-order streams combining form a third-order stream, and so on. The Nandani Watershed, characterized by a dendritic to sub-dendritic drainage pattern, emerges as a sixth-order watershed. This watershed is further subdivided into seven distinct sub-watersheds based on morphology and drainage patterns.

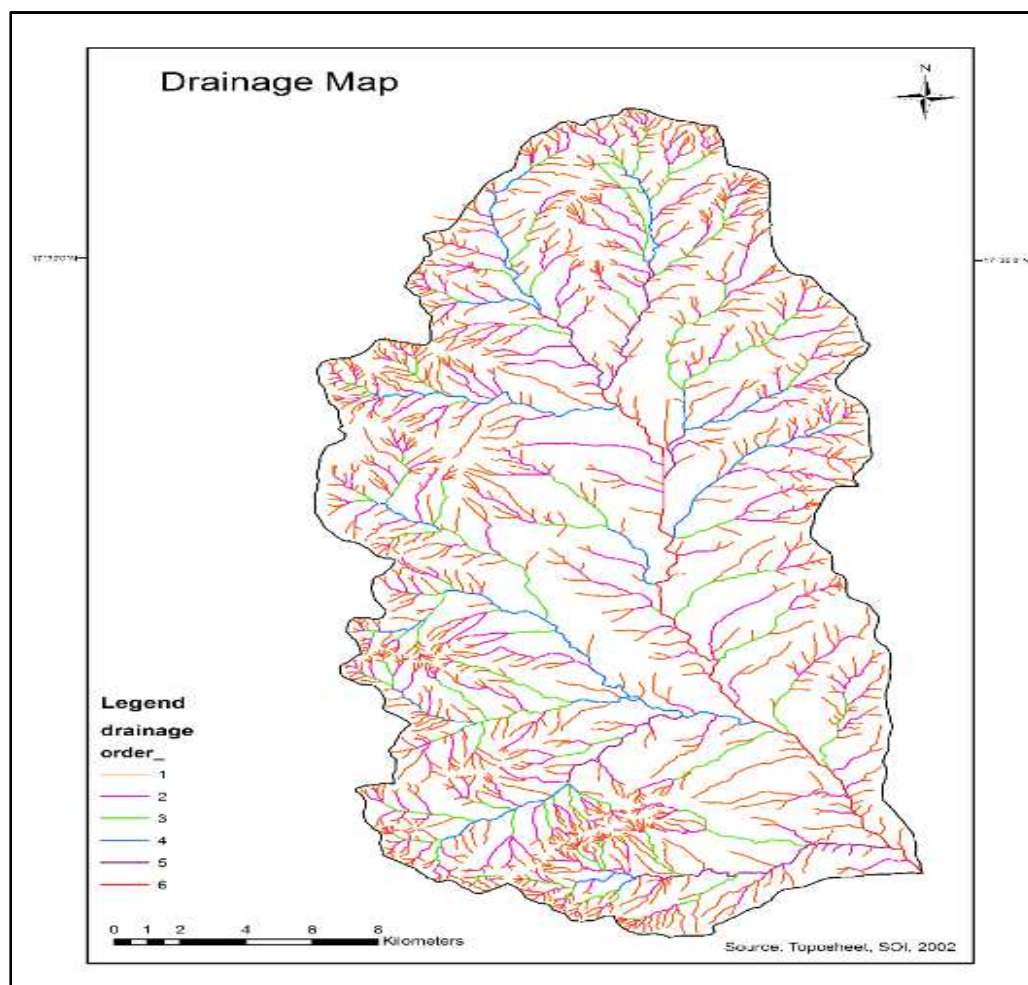


**Figure 10:** Drainage Map of Nandani Watershed

**8. Groundwater Potential Zoning:** As groundwater is not directly discernible from remotely sensed data, its presence needs to be inferred through the identification of surface features serving as indicators (Das et al. 1997; Ravindran and Jeyaram 1997). In this current study, hydro-geomorphological details, extrapolated via both visual and digital interpretation of enhanced satellite data, were harnessed to establish groundwater prospective zone maps for the study area. Hydro-geomorphological maps encompass crucial information about geomorphic units, landforms, and underlying geological attributes, contributing to an understanding of the factors influencing groundwater occurrence and potential. These maps, which outline zones with promising groundwater prospects, play a pivotal role as a foundational framework for tailored planning and localized initiatives. The groundwater potential zone map differentiates zones into categories of High, Moderate, Poor, and Very Poor, as visually represented in Figure 11. Notably, areas exhibiting high and moderate groundwater potential are prominently characterized by geomorphic units such as valley fills and pediplains, respectively. Lineaments, visually detectable surface manifestations of linear features like fractures and joints, have been extracted as linear features from imagery and subsequently verified on-site.

The delineation criteria for groundwater potential zones have been adopted from works by Krishnamurthy et al. (1992), Panigrahi et al. (1995), and Rao and Jugran (2003). The depicted groundwater potential zones in the study area are showcased in Figure 11. A significant portion of the middle section of the watershed is encompassed by zones indicating high and moderate groundwater potential. The western boundary of the study area exhibits zones denoting poor groundwater potential, primarily due to the prevalence of hills in this region. The breakdown reveals that approximately 48% of the area falls under the high potential zone, 43% under the moderate potential zone, and 9% under the poor and very poor potential zones. Examination of the groundwater potential map indicates that the most favorable groundwater potential zones are concentrated in the northeastern and northwestern regions of the study area, attributed to the presence of alluvial plains and agriculturally productive land with enhanced infiltration capacities. This method, an empirical approach combining remote sensing and GIS, effectively serves the purpose of exploring groundwater potential zones and proposing potential sites. Its applicability extends to rugged terrains over vast expanses, presenting an opportunity for exploring suitable locations.

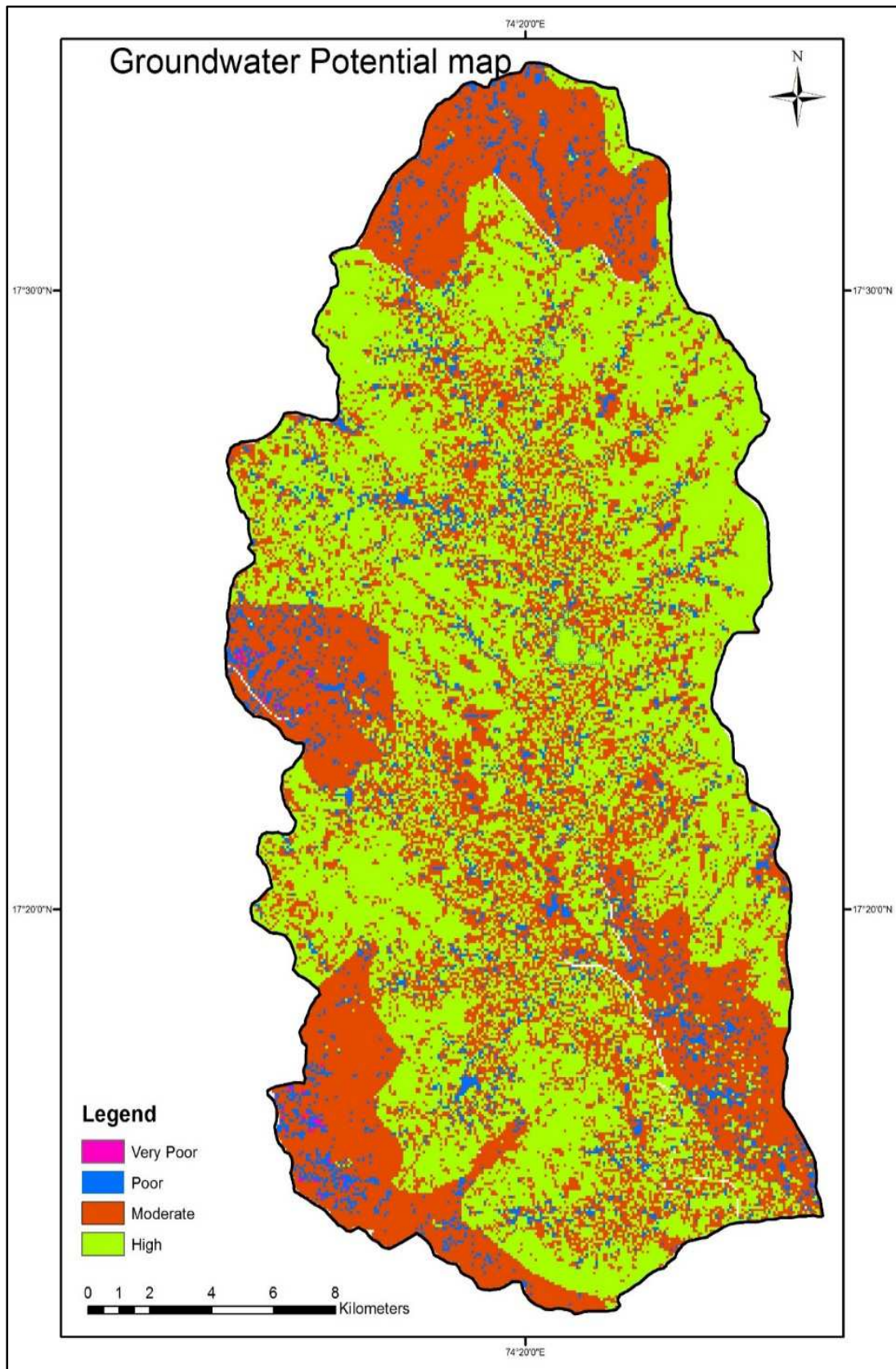


**Figure 11:** Groundwater Potential Map of the Study Area

## V. CONCLUSIONS

The primary objective of this study is to evaluate the groundwater potential zones within the Nandani watershed. To fulfill this goal, a comprehensive analysis of the Nandani watershed has been conducted, considering all feasible aspects. The groundwater potential zone map is classified into four categories: High, Moderate, Poor, and Very Poor, as visually presented in Figure 11. Within this classification, approximately 48% of the area falls under the high potential zone, 43% under the moderate potential zone, and 9% under the poor and very poor potential zones. Examination of the groundwater potential map underscores that the regions with excellent groundwater potential are concentrated in the northeastern and northwestern parts of the study area. This pattern is attributed to the presence of alluvial plains and agriculturally productive land, characterized by high infiltration capacities.

Employing an empirical approach that integrates remote sensing and GIS, this method effectively explores groundwater potential zones and suggests potential sites for groundwater zones. The versatility of this approach extends to encompass expansive areas characterized by challenging topography, thus facilitating the exploration of suitable locations.

## VI. STATEMENTS AND DECLARATIONS

The authors declare that they have no known competing financial interests or personal relationships that could have appeared to influence the work reported in this paper.

## VII. ACKNOWLEDGEMENT

The author is grateful to the Indian Metrological Department (IMD) and Survey of India (SOI) for the supply of precipitation record and toposheet.

## REFERENCES

- [1] Abdul-Aziz Hussein. Vanum Govindu. Amare Gebre Medhin Nigusse (2016), 'Evaluation of groundwater potential using geospatial techniques', *Appl Water Sci*, pp. 1-15.
- [2] Abhijit M. Zende, R. Nagarajan, K. R. Atal (2012), 'Assessment of Groundwater Potential Zones by using GIS Techniques in Yerala River Basin, Western Maharashtra, India', *International Journal of Advance Civil Engineering*, pp. 9-17.
- [3] Krishnamurthy, N. Venkatesa Kumar, V. Jayaraman And M. Manivel (1995), 'An approach to demarcate ground water potential zones through remote sensing and a geographical information system', *International Journal of Remote Sensing*, pp. 1867-1884.
- [4] M. Kavitha Mayilvaganan, P. Mohana and K.B. Naidu (2011), 'Delineating groundwater potential zones in Thurinjapuram watershed using geospatial techniques', *Indian Journal of Science and Technology Vol. 4 No. 11*, pp. 1470-1476.
- [5] N.S. Magesh, N. Chandrasekar, John Prince Soundranayagam (2012), 'Delineation of groundwater potential zones in Theni district, Tamil Nadu, using remote sensing, GIS and MIF techniques', *Geoscience Frontiers 3(2)*, pp. 189-196.
- [6] Prafull Singh, Jay Krishana Thakur & Suyash Kumar (2014), 'Delineating groundwater potential zones in a hardrock terrain using geospatial tool', *Hydrological Sciences Journal*, 58:1, pp. 213-223.
- [7] Ravindran, K.V., Jeyaram, A. (1997), 'Groundwater prospects of shahbad tehsil, baran district, eastern rajasthan: a remote sensing approach', *J Indian Soc Remote Sens* 25, pp.239-246.

- [8] S. K. Nag and Anindita Kundu (2016), 'Delineation of Groundwater Potential Zones in Hard Rock Terrain in Kashipur Block, Purulia District, West Bengal, using Geospatial Techniques', *International Journal of Waste Resources vol.6 Issue 1*, pp. 1-8.
- [9] Tesfa Gebrie Andualema, Girum Getachew Demekeb (2019), 'Groundwater potential assessment using GIS and remote sensing: A case study of Guna tana landscape, upper blue Nile Basin, Ethiopia', *Journal of Hydrology: Regional Studies 24*, pp.1-13.
- [10] Tiwari, A., Rai, B.(1996), 'Hydromorphogeological Mapping for Groundwater Prospecting Using Landsat-MSS Images — A Case Study of Part of Dhanbad District, Bihar', *J Indian Soc Remote Sens 24*, pp.281–285.
- [11] Tweed, S.O., Leblanc, M., Webb, J.A. et al.(2007), 'Remote sensing and GIS for mapping groundwater recharge and discharge areas in salinity prone catchments, southeastern Australia', *Hydrogeol J 15*, pp.75–96.
- [12] Teeuw, R.(1995), 'Groundwater Exploration Using Remote Sensing And A Low-Cost Geographical Information System', *HYJO 3*, pp.21–30.
- [13] Y. SRINIVASA RAO & D. K. JUGRAN (2003), 'Delineation of groundwater potential zones and zones of groundwater quality suitable for domestic purposes using remote sensing and GIS', *Hydrological Sciences Journal, 48:5*, pp.821-833.